Journal of Colloid and Interface Science **220,** 235–249 (1999)
Article ID jcis.1999.6501, available online at http://www.idealibrary.com on IDEAL®

Hydration and Lyotropic Melting of Amphiphilic Molecules: A Thermodynamic Study Using Humidity Titration Calorimetry

H. Binder,[1] B. Kohlstrunk, and H. H. Heerklotz*

*Universität Leipzig, Institut für Experimentelle Physik I, Linnèstr. 5, D-04103 Leipzig, Germany; and *Biozentrum der Universität Basel, Department of Biophysycal Chemistry, Klingelbergstr. 70, CH-4056 Basel, Switzerland*

Received January 19, 1999; accepted August 31, 1999

The hydration of the lipid 1-palmitoyl-2-oleoylphosphatidylcholine (POPC) and of the cationic detergent dodecyltrimethylammonium bromide (DTAB) has been studied by means of isothermal titration calorimetry (ITC), gravimetry, and infrared (IR) spectroscopy. During the experiments films of the amphiphiles are perfused by an inert gas of variable relative humidity. The measurement of adsorption heats using ITC represents a new adaptation of adsorption calorimetry which has been called the humidity titration technique. This method yields the partial molar enthalpy of water upon adsorption. It is found to be endothermic with respect to the molar enthalpy of water on condensation for the water molecules which interact directly with the headgroups of POPC and DTAB. Consequently, the spontaneous hydration of the amphiphiles is entropy driven in an aqueous environment. IR spectroscopy shows that hydration is accompanied by the increase in the conformational and/or motional freedom of the amphiphilic molecules upon water binding. In particular, a lyotropic chain melting transition is induced at a certain characteristic relative humidity. This event is paralleled by the adsorption of water. The corresponding exothermic adsorption heat is consumed completely (POPC) or partially (DTAB) by the hydrocarbon chains upon melting. Differential scanning calorimetry was used as an independent method to determine transition enthalpies of the amphiphiles at a definite hydration degree. Water binding onto the headgroups is discussed in terms of hydrogen bonding and polar interactions. The adsorption isotherms yield a number of ~2.6 tightly bound water molecules per POPC and DTAB molecule.

Key Words: **lipid membranes; water adsorption; water–headgroup interactions; enthalpy of dehydration; ITC; FTIR.**

INTRODUCTION

Amphiphilic molecules such as detergents and lipids aggregate spontaneously in an aqueous environment. The hydrated headgroups form a polar/apolar interface which screens the hydrophobic part of the molecules from the bulk water. This polar surface is an interphase rather than an interface because the polar residues are distributed throughout a meshlike region (1). It exerts a strong repulsive force toward other hydrated surfaces preventing their close attachment and fusion. Although a basic phenomenon in physical chemistry, the driving forces and structural consequences of hydration have not been understood yet in many details (2, 3). For example, hydration effects can be explained in terms of local ordering of water at the interface (4, 5) or, alternatively, as a disordering phenomenon of the headgroups which is the manifestation of the screening of inter-headgroup interactions (1, 6).

One problem arises from the fact that only rough estimates of hydration energies of amphiphiles, frequently based on theoretical calculations, are available in most cases (see Ref. (3) for an overview and references cited therein). Hence, the deficiency of experimental data impedes the quantitative estimation of the thermodynamic forces that drive the hydration of lipids and detergents.

Unfortunately, the experimental study of the thermodynamics of hydration is up to now a difficult approach because of limitations of available calorimetric methods. Considerable progress has been achieved in applying isothermal titration calorimetry (ITC) to aggregation phenomena of amphiphiles in aqueous solution during the past decade (see Ref. (7) and references cited therein) because the sensitivity of available instruments was improved drastically at the end of the 1980s (8). We have used this method by pursuing the concept of the systematic variation of the polar/apolar interface by means of the addition of detergents to lipid membranes (9, 10). The thermodynamic data could be interpreted in terms of a strong correlation between mixing properties and the hydration of the headgroups, the water exposure of the hydrophobic core, and packing effects of the hydrocarbon chains. Similar results were obtained by means of differential scanning calorimetry (DSC) in combination with infrared (IR) spectroscopy (11). Unfortunately, these investigations are restricted to excess water conditions enabling only indirect conclusions about local hydration properties.

A more direct approach to the hydration of amphiphiles is achieved when exposing the samples to an atmosphere of variable relative humidity (RH). In this way, the degree of hydration of the polar/apolar interface can be varied continu-

[1] To whom correspondence should be addressed. E-mail: binder@rz.uni-leipzig.de; Fax: 49-341-9732479.

0021-9797/99 $30.00

ously between the anhydrous and fully hydrated state of the amphiphiles. We used this sample conditioning method to study structural details of the lyotropic phase behavior of lipids by means of infrared spectroscopy and X-ray analysis (12–14). The results show that the properties of the amphiphilic aggregates decisively depend on the amount of water which forms the hydration shell.

One logical continuation of these studies was the direct measurement of hydration enthalpies using a combination of ITC instrumentation with a technique which realizes water adsorption onto amphiphiles via the gas phase (15). This experimental approach represents an adaptation of classical adsorption calorimetry. It makes use of the ability of ITC to measure mixing heats. In the usual ITC application the mixing is realized by a series of injections of a small amount of solution/dispersion from a syringe into a reaction cell containing a solution/dispersion of different composition. In analogy, our technique has been called humidity titration because "gaseous water" is "injected" in definite portions of RH to a sample film of amphiphilic molecules (15).

It is important to note that hydration affects not only the polar region of the aggregates but involves changes within the hydrophobic part as well (16). In other words, the amphiphiles represent a sorbate the properties of which vary upon sorption. That means the measured heat response yields a kind of mixing enthalpy of the two-component system sorbate (water) + sorbent (amphiphile). Consequently, the hydration of amphiphiles can be treated in analogy to the thermodynamics of two component mixtures. On the other hand, the composition, and thus the physical properties of the system, change in direction of the normal of the adsorption layer. Hence, the hydrated amphiphiles represent a mixture which is anisotropical on a microscopic length scale. A thermodynamic approach should therefore combine classical thermodynamics of binary mixtures with elements of an adsorption theory which treats, e.g., the adsorption of a sorbate in terms of distinct adsorption layers on a solid surface.

The aim of the present paper is threefold: At first we describe humidity titration calorimetry which is expected to offer new perspectives in adsorption microcalorimetry. Second, we present the basic formulae of data analysis in terms of heat contributions of the components of the system. Third, we characterize the hydration of two selected amphiphiles, the lipid POPC and the ionic detergent DTAB, in order to demonstrate the capabilities and limitations of the method and to discuss thermodynamic aspects of hydration on a molecular level.

The choice of the amphiphiles was motivated by their property to transform from a solid into a fluid state upon hydration at room temperature (17, 18). The chain melting transition represents a sort of internal heat standard. The corresponding transition enthalpy can be independently measured by DSC for the purpose of direct comparison with the ITC results. In addition, we have determined the isosteric heat of adsorption by means of gravimetry at different temperatures. IR spectroscopy is used for a qualitative characterization of intermolecular interactions.

EXPERIMENTAL

Humidity Titration Calorimetry

For sample preparation we used methanolic stock solutions (~5–20 mM) of the lipid POPC (1-palmitoyl-2-oleoylphosphatidylcholine; Avanti Polar Lipids, Birmingham, AL) and of the cationic surfactant DTAB (dodecyltrimethylammonium bromide, Aldrich, Steinheim, Germany). Definite volumes (~50 μl) were filled into the body of a cylindrical solid particle insert cell (~2 × 20 mm) of the MCS ITC calorimeter (MicroCal, Northampton, MA). The solvent was evaporated slowly under a stream of nitrogen by permanently rotating the cell. This procedure ensures the spreading of the stock solution at the inner wall of the cell. In this way the amphiphiles (~50–200 μg) are assumed to form a uniform film of a mean thickness on the order of ~1–5 μm.

The solid sample cell was thoroughly sealed and inserted through the access tube into the standard sample cell filled with water. Two steel capillaries are led out of the calorimeter through the cover of the insert cell to allow for the perfusion of the cell content. The access capillary was connected through a homebuilt adapter and a thermostated tube (flowing-water thermostat, Haake, Germany) to a moisture regulating device (HumiVar, Leipzig, Germany) that supplies a continuous flow of high-purity N_2 gas of a definite relative humidity (RH, absolute accuracy $\pm$ 0.5% at 5% $<$ RH $<$ 95%) and temperature (absolute accuracy $\pm$ 0.1 K, short-time stability $< \pm 10^{-2}$ K). The gas passes through the access capillary and, additionally, pre-equilibrates thermally before it enters the cell (temperature stability $< \pm 10^{-3}$ K). After flowing over the sample film, the nitrogen and the surplus vapor leave the cell through the outlet capillary into the room atmosphere.

The samples were investigated by means of increasing (hydration scan) as well as decreasing (dehydration scan) RH at $T = 25$°C. The RH was varied between 2 and 92% in steps of ΔRH = 2% (see Fig. 1 for illustration). Practically, the RH jumps were realized abruptly ($t_{step} \approx 20$ s) when compared with the response time of the sample (see below). The RH was adjusted with a stability of $<\pm 0.15$% in the interval between two steps as has been checked by means of a capacitive RH sensor (cf. Fig. 1).

The change of RH typically results in the sorption/desorption of water onto/from the sample film. The corresponding heat of adsorption is detected as a power peak of the cell feedback circuit (CFB) to balance temperature differences between the sample and the reference cell, both residing within an adiabatic jacket. The time interval between two subsequent RH steps ($t_{wait} \approx 15$ min) was chosen to exceed the characteristic relaxation time of the system ($\tau_{eq} < 5$ min) to ensure

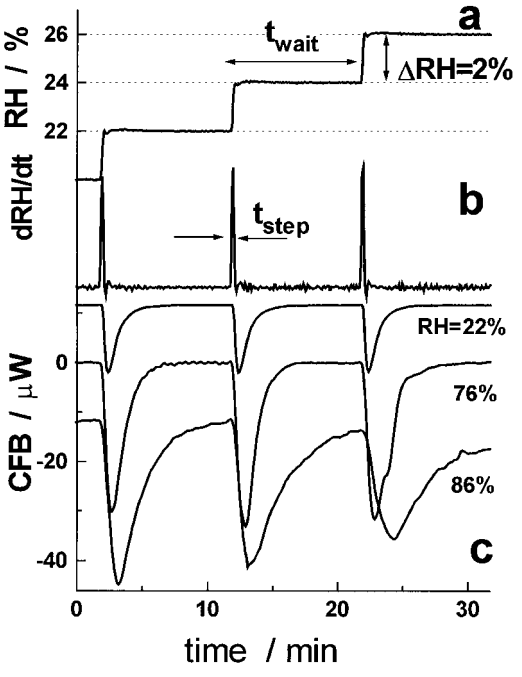

FIG. 1. Humidity titration calorimetry: Relative humidity (RH) (a), their derivative (b), and the power peaks of the cell feedback circuit (CFB) (c) measured upon hydration of POPC as a function of time. The three curves depicted in (c) correspond to different RH ranges starting with the RH value given at the plots. A capacitive sensor (Vaisala, Finnland) has been used for the determination of RH of the gas immediately before it enters the calorimeter cell.

reequilibration after sorption (see Fig. 1). The equilibration time, τ_{eq}, is nearly independent of the flow rate of the gas, ν_{flow}, when choosing ν_{flow} in the interval $\nu_{flow} \approx (10–50)$ μl/s. At smaller flow rates, the width of the CFB pulses increases considerably, obviously, because the transport of the sorbate into the sample cell becomes rate limiting. Note, that $\nu_{flow} = 10$ μl/s realizes the access of $\sim 2 \times 10^{-8}$ mol water/s at RH = 98%. This amount of water corresponds to ~1% of the respective hydration capacity of 100 μg of a lipid (~12 mol water/mol lipid, see below).

In a series of preexperiments, we varied the amount of sample in the range $m_{sample} = (50–400)$ μg. It turns out that τ_{eq} and the integrated heat of the CFB pulses per mol of sorbent are essentially independent on m_{sample} at $m_{sample} < 400$ μg. τ_{eq} increases typically with increasing RH from, e.g., less than 2 min at RH < 22% to ~10 min at RH > 85% for POPC (see Fig. 1). A similar tendency has been reported previously by equilibrating lipids in a humid atmosphere (17). The slowing-down of the heat response also occurs when the sample passes a melting transition. A reference measurement using an empty insert cell shows that background effects can be neglected (Fig. 4).

Gravimetric Measurements

The surfactant in methanolic stock solution (~0.5 ml) was spread on the surface of a circular quartz slide (diameter 15 mm) and allowed to dry under a stream of nitrogen. The sample was placed into a twin microbalance system (Sartorius, Germany) which has been equipped with a moisture regulating device (see above and (12)). The relative humidity was adjusted by flowing moist, high-purity N_2 gas through the sample chamber. Before starting the experiments, the surfactant was dried by flowing dry N_2 for 12–24 h through the chamber (T = 25°C) until the mass of the sample attained some constant value (~0.5 mg). Infrared spectra of lipid films which were incubated at identical conditions show nearly no absorption in the spectral range of the ν_{13}(OH) stretching band of water (vide infra). We cannot exclude, however, that 1–2 "invisible" water molecules remain strongly bound after drying. Note that the calorimetric data were calibrated using the incremental adsorption of water ($R'_{W/L}$, cf. Eq. [4] below) instead of the molar ratio water-to-lipid ($R_{W/L}$). Consequently, the absolute amount of adsorbed water is of less importance in this context. The integral enthalpy, entropy, and free enthalpy of complete dehydration (vide infra) and the $R_{W/L}$ scale used refer to the described drying procedure.

Adsorption isotherms were recorded in the continuous mode by scanning the RH with a constant rate of $<\pm 10\%$ per hour throughout the range 0–98% and recording the mass increment. The samples were investigated by means of increasing (hydration scans) as well as decreasing (dehydration scan) RH at constant temperature in analogy to the ITC experiments.

Infrared and DSC Measurements

Films of the amphiphiles were prepared on the surface of a ZnSe-attenuated total reflection (ATR) crystal using the same procedure, solvent, and conditions as described above. The samples for ITC, gravimetry, and FTIR measurements are assumed to possess virtually identical physicochemical properties owing to the very similar conditions of preparation. The ATR crystal was mounted into a BioRad FTS-60a Fourier transform infrared spectrometer (Digilab, MA) using a commercial horizontal Benchmark unit (Graseby Specac, U.K.) which has been modified to realize a definite relative humidity (RH) and temperature at the crystal surface coated with the sample (12). Absorption spectra were recorded as a function of RH in steps of 3% at constant temperature.

For DSC measurements ~10 mg of the amphiphiles were hydrated by adding a constant amount of water (see below). Measurements were performed with a Perkin–Elmer DSC-7 instrument (Germany) using heating and cooling rates of 1–2 K/min. The transition enthalpies, ΔH_m^{DSC}, were obtained by integrating the thermograms over the phase transition range.

THEORY

Observed Heats and the Enthalpy of Dehydration

We consider an ensemble of N_L moles of hydrated amphiphilic molecules under isothermal and isobaric conditions in

an atmosphere of vapor pressure p which represents the sorbate + sorbent system within the sample cell of the calorimeter. Assuming an ideal gas phase and choosing the atmosphere at saturation pressure, p_0, as reference state, then the activity of the water is defined by $a_W \equiv p/p_0 = \mathrm{RH}/(100\%)$. The change of a_W induces the variation of the number of moles of water adsorbed onto the sample:

$$\Delta N_W^{g\to s} = N_L \cdot \Delta R_{W/L} = N_L \cdot R'_{W/L} \cdot \Delta a_W. \qquad [1]$$

$R_{W/L}(a_W) = N_W/N_L$ represents the adsorption isotherm of water and $R'_{W/L} = (\partial R_{W/L}/\partial a_W)$ its slope. The change of the enthalpy of the sample which is caused by the variation of a_W is given by

$$\Delta H_{sample}(a_W) = \frac{\partial H_{sample}}{\partial a_W} \cdot \Delta a_W = \frac{\partial H_{sample}}{\partial N_W} \cdot \Delta N_W^{g\to s}. \qquad [2]$$

The derivative $\partial H_{sample}/\partial N_W \equiv h_W^s$ is the partial molar enthalpy of water in the adsorbed state.

The heat, Q, consumed (>0) or released (<0) upon reequilibration of the system sorbent + sorbate after changing a_W is just the enthalpy difference between the previous and the new equilibrium state of the sample minus the enthalpy change of the gaseous water which is sorbed:

$$Q = \Delta H_{sample} - \Delta H_{gas}. \qquad [3]$$

With $\Delta H_{gas} = \Delta N_W^{g\to s} \cdot h_W^g$ and making use of Eq. [2] one obtains after normalization with respect to the experimental input, $N_L \cdot \Delta a_W$,

$$q_{ITC} \equiv \frac{1}{N_L} \cdot \frac{Q}{\Delta a_W} = R'_{W/L} \cdot \Delta h_W^{g\to s}. \qquad [4]$$

The difference of the partial molar enthalpy of water upon transfer from the gas into the sorbed phase is defined as $\Delta h_W^{g\to s} \equiv h_W^s - h_W^g$. The partial molar enthalpy of the vapor, h_W^g, is independent of RH when assuming an ideal gas phase, i.e., $h_W^g = \text{const}$. Integration yields the total heat of adsorption per mole of sorbent

$$Q_{ITC}(a_W) \equiv \int_0^{a_W} q_{ITC} \cdot da_W. \qquad [5]$$

Rearrangement of Eq. [4] yields

$$\Delta h_W^{g\to s} = \frac{Q}{\Delta N_W^{g\to s}} = \frac{q_{ITC}}{R'_{W/L}} \qquad [6]$$

which represents the heat per mole sorbate which is transferred to the surroundings upon transferring of a differential quantity of sorbate from the vapor phase to the adsorbed phase.

Amphiphiles are usually studied under excess water conditions. It is therefore convenient to calculate the enthalpy change of water, $\Delta h_W^{b\to s}$, upon transfer from the aqueous bulk phase into the hydration shell of the amphiphiles

$$\boxed{\Delta h_W^{b\to s} = \Delta h_W^{g\to s} - \Delta h_W^{g\to b}} \qquad [7]$$

where $\Delta h_W^{g\to b} = h_W^b - h_W^g$ denotes the condensation heat of (bulk) water (e.g., ~ -44.6 kJ/mol at $T = 25°C$). The integrated heat of dehydration is given by

$$\boxed{\Delta H^{s\to b}(a_W) \equiv \int_1^{a_W} \Delta h_W^{b\to s} \cdot R'_{W/L} \cdot da = \Delta Q_{ITC}^{s\to b}(a_W) - \Delta h_W^{g\to b} \cdot \Delta R_{W/L}^{s\to b}(a_W)} \qquad [8]$$

with $\Delta R_{W/L}^{s\to b}(a_W) \equiv R_{W/L}(a_W) - R_{W/L}(1)$ and $\Delta Q_{ITC}^{s\to b} \equiv Q_{ITC}(a_W) - Q_{ITC}(1)$. Note that $\Delta H^{s\to b}$ and $\Delta h_W^{b\to s}$ refer to opposite directions of the transfer of water. The enthalpy of dehydration, $\Delta H^{s\to b}$, gives the overall enthalpic effect per mole amphiphile when (hypothetically) reducing the hydration shell by transferring the adsorbed water into the bulk water. It can be illustrated in terms of a two-step transfer of water including (i) the desorption from the sorbed into the gas phase and (ii) the subsequent condensation onto bulk water (cf. Fig. 2).

Free Enthalpy of Dehydration

The chemical potential of the water adsorbed onto the amphiphile is adjusted by the activity of the vapor surrounding the sample, $\mu_W = \mu_W^s = \mu_W^g$:

$$\mu_W \equiv N_L^{-1} \cdot \left(\frac{\partial G_{sample}}{\partial R_{W/L}}\right)_{\substack{T=\text{const}\\ p=\text{const}}} = \mu_W^b + RT \cdot \ln a_W. \qquad [9]$$

R denotes the gas constant and μ_W^b is the chemical potential of saturated vapor which is equal to that of bulk water. Following the same logic as in the previous paragraph one obtains the free enthalpy of dehydration per mole amphiphile (3).

$$\Delta G^{s\to b}(a_W) = RT \cdot \int_1^{a_W} \ln a_W \cdot R'_{W/L} \cdot da_W \qquad [10]$$

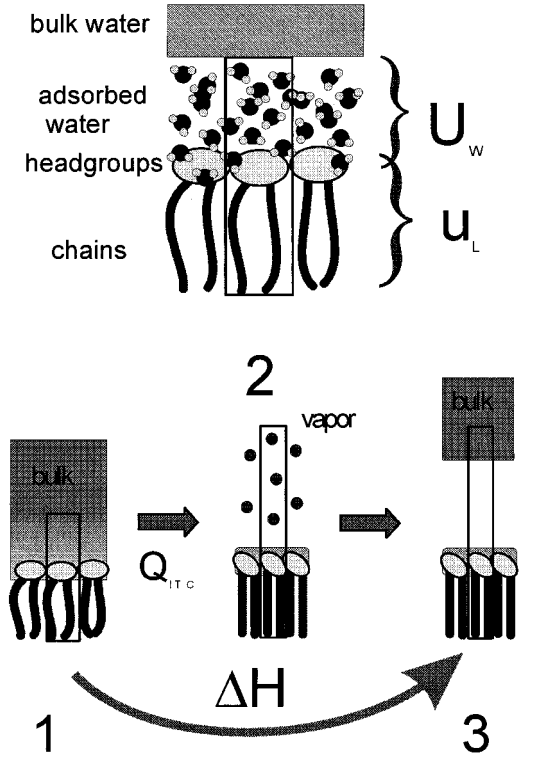

FIG. 2. Schematic illustration of a fully hydrated lipid layer (above, see text) and of the heat contributions to the enthalpy of dehydration, $\Delta H^{s\to b}$ (below). (1) Fully hydrated amphiphile in equilibrium with bulk water; (2) desorption of $\Delta R_{W/L}$ water molecules per amphiphile into the gas phase; (3) (hypothetical) condensation of the vapor onto bulk water. The heats ΔQ_{ITC} and $\Delta R_{W/L} \cdot \Delta h_W^{g\to b}$ release at the first and second step within the sequence (1) $\to$ (2) $\to$ (3), respectively, whereas $\Delta H^{s\to b}$ gives the enthalpy of the direct transformation between (1) and (3). The rectangle encloses a constant amount of material which yields the heat contributions, namely one amphiphile plus the amount of adsorbed water at full hydration.

Making use of

$$\Delta G^{s\to b} = \Delta H^{s\to b} - T \cdot \Delta S^{s\to b} \qquad [11]$$

($\Delta S^{s\to b}$ is the corresponding entropy change), of $\Delta\mu_W^{b\to s} = -\partial(\Delta G^{s\to b})/\partial R_{W/L}$, and of $\Delta h_W^{b\to s} = -\partial(\Delta H^{s\to b})/\partial R_{W/L}$ one obtains after differentiation of Eq. [9] at $R_{W/L} = \text{const}$

$$\Delta h_W^{b\to s} = \left(\frac{\partial(\Delta\mu_W^{b\to s}\cdot T^{-1})}{\partial T^{-1}}\right)_{R_{W/L}=\text{const}} = R\cdot\left(\frac{\partial \ln a_W}{\partial T^{-1}}\right)_{R_{W/L}=\text{const}}. \qquad [12]$$

Note that $h^{iso}(a_W) = -\Delta h_W^{b\to s}$ is commonly referred to as the isosteric heat of adsorption (19, 20). Hence, gravimetric measurements at different temperatures reveal an independent method to determine the change of the partial molar enthalpy of water on hydration.

Enthalpic Contributions of the Components

Let us decompose the enthalpy of the sample, H_{sample}, into contributions of the amphiphile and the water in analogy to a binary mixture (10):

$$H_{sample}(a_W) = N_L \cdot (h_L(a_W) + R_{W/L}(a_W)\cdot h_W^s(a_W)). \qquad [13]$$

$h_L \equiv \partial H_{sample}/\partial N_L$ and h_W^s are defined as the partial molar enthalpies of the components. One should note that h_L and h_W^s are not independent of each other. Differentiation of Eq. [13] with respect to $R_{W/L}$ yields $\partial h_L/\partial R_{W/L} = -R_{W/L}\cdot\partial h_W^s/\partial R_{W/L}$. Integration of $\partial\Delta h_W^{b\to s}/\partial R_{W/L} = \partial h_W^s/\partial R_{W/L}$ gives the difference of h_L between the fully and partially hydrated state:

$$\Delta h_L^{b\to s} \equiv h_L(a_W) - h_L(1) = -\int_{R_{W/L}(1)}^{R_{W/L}(a_W)} R_{W/L}\cdot\frac{\partial\Delta h_W^{b\to s}}{\partial R_{W/L}}\, dR_{W/L}. \qquad [14]$$

Note that $\Delta h_L^{b\to s}$ refers to the removal of adsorbed water from the amphiphile. The fully hydrated state is defined by the condition of phase coexistence between the hydrated amphiphiles and bulk water at $a_W = 1$. The partial molar enthalpies of bulk and bound water can differ at full hydration, i.e., $h_W^s(1) \neq h_W^b$, in contrast to the chemical potential of water which is equal in the coexisting phases, i.e., $\mu_W^s(1) = \mu_W^b$.

Figure 3 illustrates the correlation between $\Delta h_L^{b\to s}$ and $\Delta h_W^{b\to s}$ as a function of $R_{W/L}$ for several characteristic cases. Figure 3a refers to continuous (e.g., exponential) and Fig. 3b to stepwise changes of $\Delta h_W^{b\to s}$ and $\Delta h_L^{b\to s}$. The latter situation should apply to hydration in terms of discrete adsorption layers. Figures 3c and 3d show the expected changes of $\Delta h_L^{s\to b}$ and of $\Delta h_W^{b\to s}$ when the amphiphile undergoes a lyotropic phase transition (see

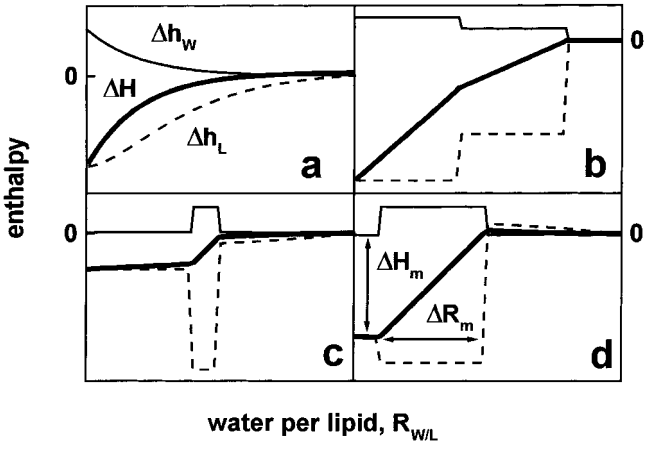

FIG. 3. Schematic illustration of the correlation between the partial molar transfer enthalpies of the water, $\Delta h_W^{b\to s}$ (solid line), of the amphiphile, $\Delta h_L^{b\to s}$ (dashed line), and of the enthalpy of dehydration, $\Delta H^{s\to b}$, (thick solid line, Eq. [8]) in four characteristic cases (see text).

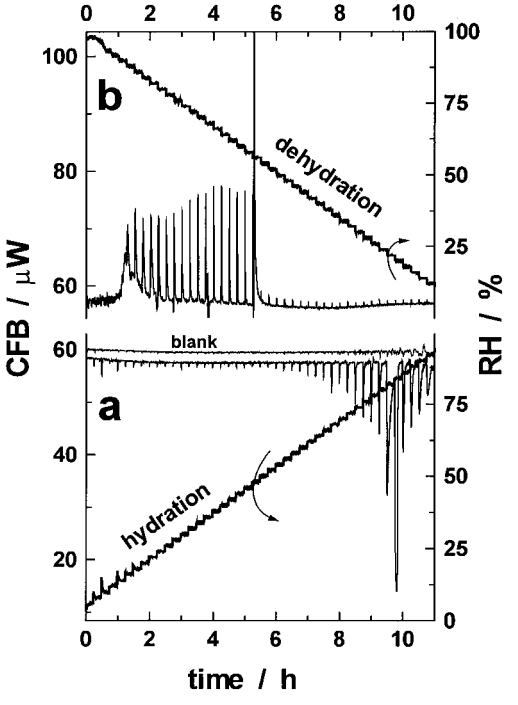

FIG. 4. Experimental raw data collected by a humidity titration experiment: RH "staircase" (right axes) and the CFB pulses caused by the hydration (a) and dehydration (b) of 45 μg DTAB at $T = 25$°C. The CFB response of a blank experiment are shown in (a).

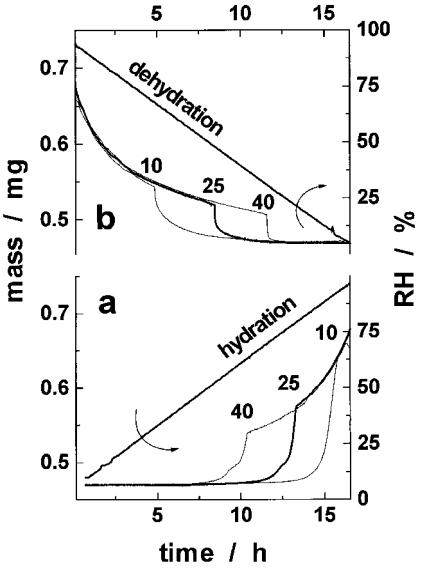

FIG. 5. Experimental raw data collected by gravimetry: RH ramp (right axes) and mass of DTAB + adsorbed water at increasing (a) and decreasing (b) RH at $T = 10$, 25, and 40°C.

below). For sake of simplicity, we have assumed that the enthalpy of water binding remains unchanged before and after the phase transition where $\Delta h_W^{b\to s}$ is slightly positive (3c) or negative (3d). Figures 3c and 3d mainly differ in the amount of water, ΔR_m, adsorbed at the phase transition.

RESULTS

Water Adsorption and Measured Heats

Figure 4 depicts typical raw data obtained in the humidity titration experiment. Each jump of RH causes a CFB pulse which is endothermic upon dehydrating and exothermic upon hydrating the sample. Integration of the pulses yields the heat, q_{ITC}, released (hydration) or consumed (dehydration) in each RH step (see Fig. 6a).

Figure 5 displays the raw data of the corresponding gravimetric experiment and Fig. 6b the corresponding adsorption isotherms. Its first derivative, $R'_{W/L}$, is proportional to the number of water molecules adsorbed/desorbed from the sample at a given RH. The virtually parallel dependencies of $R'_{W/L}$ and of q_{ITC} (cf. Fig. 6) indicate that the shape of $q_{ITC}(a_W)$ is mainly determined by $R'_{W/L}$ and only to a less extent by the change of the partial molar enthalpy of water upon adsorption, $\Delta h_W^{g\to s}$ (cf. Eq. [4]).

At low and intermediate RH, the detergent, DTAB, forms nearly anhydrous, crystalline lamellae where the all-*trans* alkyl chains pack into a paraffin-like structure (18). The variation of RH has essentially no effect on $R_{W/L}$ and consequently the heat response of the sample is very small. At a threshold value of RH, the solid surfactant melts. This event is paralleled by the adsorption of 2–3 water molecules per DTAB molecule causing intense exothermic CFB pulses. In accordance with the phase diagram of dodecyltrimethylammonium chloride, we

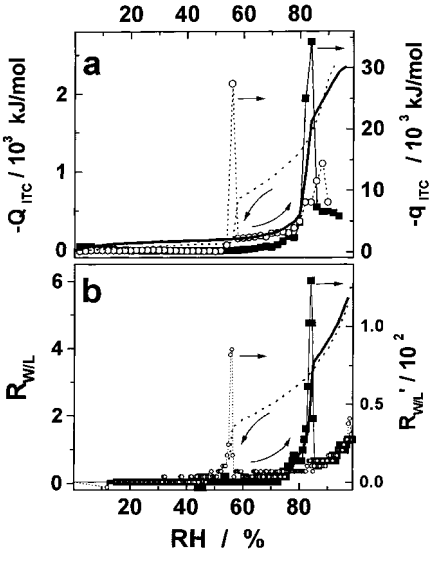

FIG. 6. Measured heats, q_{ITC} (a, symbols), and molar ratio water per amphiphile, $R_{W/L}$ (b, lines), of DTAB at $T = 25$°C as a function of RH upon hydration (solid lines) and dehydration (dotted lines). The integrated heat of sorption, Q_{ITC} (lines), and the first derivative of $R_{W/L}$, $R'_{W/L}$ (symbols), are also shown in (a) and (b), respectively.

assign the liquid state of DTAB to a nonlamellar, hexagonal "middle" phase where cylindrical micelles align parallelly with their long axes (21).

The calorimetric and gravimetric dehydration scans reveal a considerable hysteresis when compared with the hydration scans. The sample undergoes the freezing transition at a RH which is distinctly reduced in comparison with that of the melting transition. The formation of crystalline structures of long chain amphiphiles is typically accompanied by marked nonequilibrium effects such as "phase transitions upon storage" and freezing/melting hystereses (12, 22–24). We did not study this effect systematically by, e.g., the variation of the scan rate, because the phase behavior of DTAB in thermodynamic equilibrium is not in the center of interest of the present investigation. FTIR measurements on DTAB spread on a ZnSe crystal show a melting/freezing hysteresis at RH = 69/75% (18), i.e., at a position which is intermediate between the melting and freezing humidity obtained by means of gravimetry and ITC. We suggest that melting and freezing are delayed and/or shifted in these experiments owing to unknown factors. Note that also DSC heating and cooling scans of partially hydrated DTAB show a considerable melting/freezing hysteresis of more than 15 K (see below, Table 2). From a methodical point of view the hysteresis attracts interest because the ranges of weak and stronger hydration of DTAB extend to higher and lower RH in the hydration and dehydration scans, respectively. In this way, metastability effects of water adsorption and desorption can be judged thermodynamically.

The lipid POPC continuously adsorbs water throughout the whole RH range. After the initial binding of ~1 water molecule at RH < 10%, the lipid swells already in the gel state and, thus, each RH step gives rise to a considerable CFB pulse (cf. Fig. 1). No significant hysteresis effects could be detected in the corresponding dehydration scan (not shown). The adsorption isotherm shows the typical shape which has been reported previously for lipids with PC headgroups (25) (Fig. 7b).

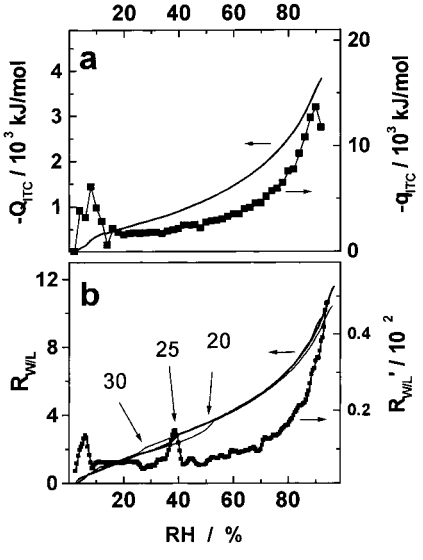

FIG. 7. Measured heats, q_{ITC} (a), and molar ratio water per amphiphile, $R_{W/L}$ (b), of POPC at T = 25°C as a function of RH. See legend of Fig. 6 for assignments. The thin lines in (b) denote isotherms which are recorded at T = 20 and 30°C.

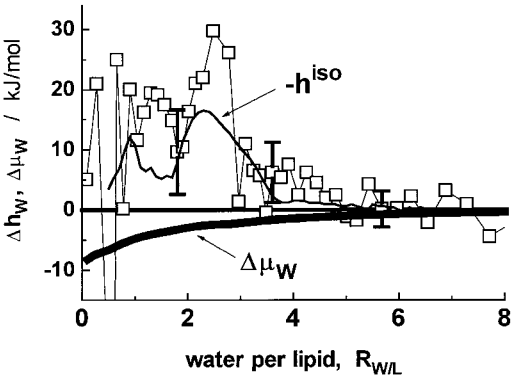

FIG. 8. Partial molar transfer enthalpy $\Delta h_W^{b\to s}$ (open squares, cf. also Eqs. [6] and [7]) and chemical potential of water $\Delta\mu_W^{b\to s}$ adsorbed on to POPC as a function of water molecules per amphiphile, $R_{W/L}$ (T = 25°C). The solid curve depicts the isosteric heat of adsorption, $-h^{iso}$ (cf. Eq. [12]).

The slight step of $R_{W/L}$ at RH ≈ 40% is caused by the lyotropic chain melting transition of POPC which transforms from the gel into the liquid-crystalline phase (17). Note that this detail of the adsorption isotherm has not been detected in a previous study on water adsorption onto POPC where RH has been adjusted using saturated salt solutions (26). The RH-dependence of the integrated pulses, q_{ITC}, resembles closely that of $R'_{W/L}$ as in the case of DTAB (cf. Fig. 7). The phase transition of the lipid proceeds, however, without significant heat effects (compare Figs. 7a and 7b). The condensation heat of the water which is imbibed by the lipid at the phase transition obviously completely compensates the heat which is consumed by the chains upon melting (vide infra).

The phase transitions of DTAB and POPC shift to smaller RH values with increasing temperature (cf. Figs. 4 and 6).

Enthalpy and Entropy of Dehydration

Figure 8 depicts the partial molar transfer enthalpy of water on hydration, $\Delta h_W^{b\to s}$, of POPC and Fig. 9 the enthalpy of dehydration, $\Delta H^{s\to b}$, of both amphiphiles as a function of $R_{W/L}$. No significant enthalpic effects exceeding the condensation heat of water could be detected in the ITC experiment at $R_{W/L} > 4$–5 (hydration scan) and >2 (dehydration of DTAB), i.e., $\Delta h_W^{b\to s} \approx -\Delta H^{s\to b} \approx 0 \pm 4$ kJ/mol. However, $\Delta h_W^{b\to s}$ increases distinctly upon further dehydration of the lipid. Hence, the transfer of water from the bulk into the hydration shell of POPC is endothermic. The corresponding integrated heat of dehydration, $\Delta H^{s\to b}$, gets negative because the system (hydrated amphiphile + bulk water) gains enthalpy when water is released from the sorption layer into the bulk (cf., Fig. 9). Note that the enthalpy functions of POPC can be understood as

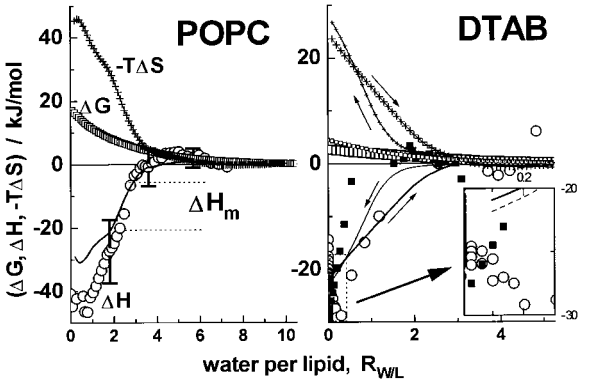

FIG. 9. Free energy, enthalpy, and entropy of dehydration of POPC and DTAB as a function of the molar ratio water-to-amphiphile, $R_{W/L}$. The enthalpy, $\Delta H^{s\to b}$ (circles), and the free enthalpy, $\Delta G^{s\to b}$ (squares), were determined by means of ITC and gravimetric measurements at $T = 25$°C (Eqs. [8] and [10], resp.). Alternatively $\Delta H^{s\to b}$ (lines) and the corresponding entropic term, $-T\Delta S^{s\to b}$ (crosses), were calculated from the adsorption isotherms measured at $T = 25$ and 40°C (DTAB) and at 20 and 30°C (POPC) (cf. Eqs. [11] and [12]). Small symbols and the thin lines in the right part (DTAB) correspond to the dehydration scan. The inset in the right part enlarges the range $R_{W/L} < 0.3$ as indicated.

a superposition of the schematic dependencies shown in Figs. 3a and 3c whereas $\Delta H^{s\to b}$ of DTAB qualitatively resembles the respective curve in Fig. 3d.

For an independent determination, we have calculated $\Delta h_W^{b\to s}$ and $\Delta H^{s\to b}$ by means of the isosteric heat of adsorption using the adsorption isotherms of DTAB at $T = 25$ and 40°C and that of POPC at $T = 20$ and 30°C (cf. Eq. [12] and lines in Figs. 8 and 9). The variation of $R_{W/L}$ with temperature is rather weak except the shift of the RH jump which is observed at the phase transition (cf. Figs. 5 and 7). To estimate the accuracy of the measurement in terms of enthalpy, let us assume a constant uncertainty of δRH $\approx \pm 1\%$ for the isotherms measured. This error of RH entails an error of the isosteric heat of $\delta h^{iso} \approx \pm 1$ kJ/mol at RH = 80% and of $\delta h^{iso} \approx \pm 5$ kJ/mol at 20% for the temperature interval of (10–15)K in which $\Delta h_W^{b\to s}$ is assumed to be a constant. The agreement between the results of the direct and indirect determination of $\Delta h_W^{b\to s}$ and $\Delta H^{s\to b}$ by means of ITC and temperature variation is satisfactory in view of this uncertainty.

The chemical potential of hydration, $\Delta\mu_W^{b\to s}$, is given by the adsorption isotherms (cf. Eq. [9] and Fig. 8 for POPC). Integration yields the free energy of dehydration, $\Delta G^{s\to b}$, and the entropic contribution, $-T \cdot \Delta S^{s\to b}$ as a function of $R_{W/L}$ (Fig. 9 and Eqs. [10] and [11]). The negative slope of $-T \cdot \Delta S^{s\to b}$ indicates that hydration is entropically driven for the amphiphiles investigated. From the measurement of the isosteric heats of lecithins Elworthy concluded 37 years ago that mixing effects between the sorbed water and the polar headgroups predominates over any effect due to a specific arrangement of water molecules near these groups (20). Beside this mixing entropy also the configurational disordering of the headgroups (13, 27) and the melting of the hydrocarbon chains (see below) are expected to increase the entropy upon hydrating amphiphilic molecules.

Hydration Sites and Molecular Order: Infrared Measurements

Among other factors, the frequency of a stretching vibration depends on the molecular conformation and on the intermolecular potential which acts on the vibrating atoms. Consequently, infrared spectroscopy provides microscopic information about the structure and specific interactions within molecular assemblies of long chain amphiphiles at hydration/dehydration (12, 14, 18).

For example, the marked frequency increase in the antisymmetric methylene stretching band, $\nu_{as}(CH_2)$, of DTAB and POPC represents a diagnostic signature of the chain melting transition (28, 29) (see Fig. 10). The frozen alkyl chains of DTAB adopt the extended all-*trans* conformation and arrange densely into an orthorhombic perpendicular packing mode in the solid state (18). The regular packing of the acyl chains of solid POPC is perturbed by several effects. First, both chains of each lipid molecule are subjected to restrictions of their conformation near their linkage to the glycerol moiety (30). Second, the *cis*-double bonds give rise to a considerable residual conformational disorder of the polymethylene segments of the oleoyl chain which are not strictly all-*trans* and, furthermore, are prevented from arranging together with the palmitoyl

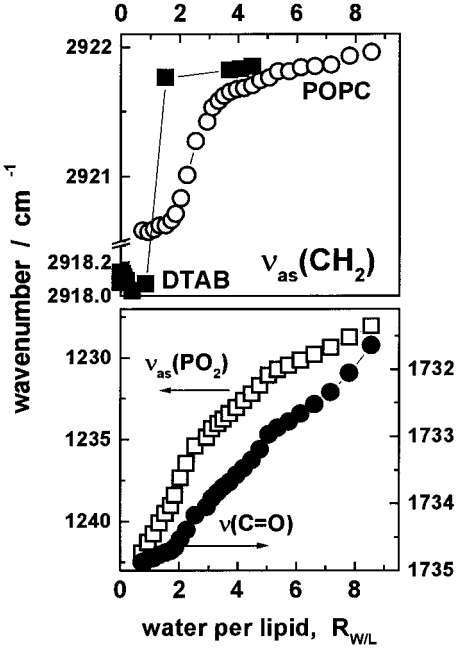

FIG. 10. Position of the antisymmetric methylene stretching band, $\nu_{as}(CH_2)$ (a), of POPC (open symbols) and DTAB (solid) and the position of the antisymmetric phosphate, $\nu_{as}(PO_2^-)$ (open), and of the carbonyl, $\nu(C=O)$ (solid), stretching bands of POPC (b) as a function of the number of water molecules bound per lipid. The wavenumbers were calculated by means of the center of gravity of the respective absorption bands (12).

chains into a paraffin-like structure (31). The gel-like character of the solid lipid is reflected in the wavenumber of the $\nu_{as}(CH_2)$ band which is shifted by $\sim$2.5 cm^{-1} to larger values when compared with that of crystalline DTAB (Fig. 10). An upward shift of the $\nu_{as}(CH_2)$ band can be interpreted in terms of decreased attractive interactions between the hydrocarbon chains (32). Following this interpretation the slight increase of $\nu_{as}(CH_2)$ in the gel and liquid-crystalline phases of POPC with increasing hydration reflects the weakening of intermolecular interactions and the gradual decrease in the degree of conformational order (see below).

The positions of the antisymmetric PO_2^- and of the C = O stretching bands, $\nu_{as}(PO_2^-)$ and ν(C = O), respectively, can be interpreted as a qualitative measure of hydrogen bonding between water and the phosphate and carbonyl groups, respectively (33, 34). The almost regular variation of the position of both bands indicates that the degree of water–phosphate and of water–carbonyl interactions changes continuously throughout the whole range of water adsorption onto POPC. The steeper slope of $\nu_{as}(PO_2^-)$ at $R_{W/L} < 3$ can be attributed to the high affinity of the phosphate group to the adsorption of water. The phase transition of POPC only weakly affects the polar moieties. A certain shielding of the C = O group from the water in the gel state can be deduced from the break of the ν(C = O) course at the onset of the chain melting transition in agreement with the results of IR investigations on lipids at full hydration (11).

The width and position of the OH stretching band of water, ν_{13}(OH), adsorbed onto lipids yield qualitative information about water–lipid interactions (12). An unambiguous interpretation of the ν_{13}(OH) band is difficult because its shape and frequency can reflect (i) different energetic characteristics of adsorbed water molecules, (ii) intra- and intermolecular couplings between the OH stretching vibrations, and/or (iii) Fermi resonance with $2 \cdot \nu_2$, the H–O–H bending mode (35, 36). The vibrational mixing can be eliminated to a great extent by means of isotopic dilution of H_2O by D_2O. The low-frequency shoulder of the ν_{13}(OH) band ($\sim$3270 cm^{-1}) of H_2O adsorbed onto POPC disappears completely in a mixed vapor atmosphere of composition H_2O/D_2O = 1:10 (mol/mol). We conclude that this feature is caused by vibrational coupling and, thus, reflects properties of the water structure. A similar conclusion has been drawn on the basis of the IR linear dichroism of the ν_{13}(OH) band of water adsorbed onto a PC headgroup (13). On the other hand, the maximum position of the ν_{13}(OH) band near 3400 cm^{-1} remains unaffected by isotopic dilution (cf. Figs. 11b and 11c). Consequently, this frequency is assumed to give a rough measure of the strength of water binding. The maximum shifts to smaller wavenumbers by about 20 cm^{-1} at dehydration, suggesting stronger water–headgroup interactions when compared with water–water interactions (Figs. 11b and 11c). The slight narrowing of the band reflects, possibly, the narrowing of the distribution of the respective interaction energies.

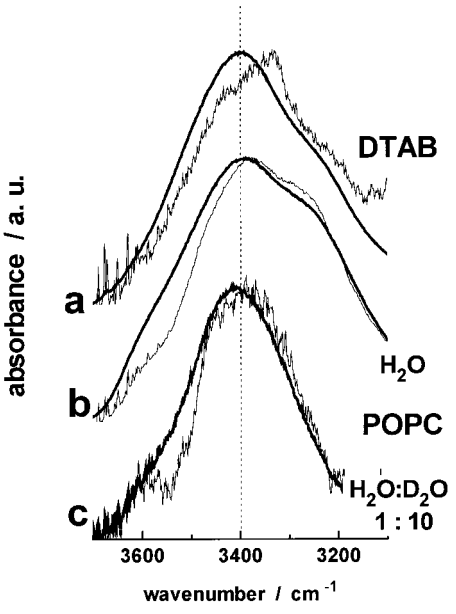

FIG. 11. Normalized absorbance spectra of the OH stretching region of water bound to DTAB (a) and POPC (b and c). Thin and thick lines correspond to the solid and liquid states of the amphiphiles with $R_{W/L} \approx 0.5$ and 5 (DTAB) and $R_{W/L} \approx 1$ and 10 (POPC), resp. (c) corresponds to the same conditions as (b) except the composition of the atmosphere surrounding the sample which has been modified as indicated in the figure.

The maximum intensity of the ν_{13}(OH) band is significantly enhanced relative to the shoulder near 3270 cm^{-1} when water is adsorbed onto DTAB (cf. Fig. 11a). This effect can be interpreted in terms of the partial breakdown of the water structure (37). Note that hydrogen bond formation between water and the $N^+(CH_3)_3$ site cannot occur. Instead, the water dipoles are expected to associate with the charged trimethylammonium (TMA) moieties via weaker polar interactions (38). The bandshape remains nearly constant upon dehydration except a feature near 3330 cm^{-1} which appears at a very low level of hydration ($R_{W/L} < 0.5$). It originates probably from vibrations of $Br^- \cdots$ H–O units (37).

The conformation of the C–C–$N(CH_3)_3$ fragment of DTAB in the crystalline state is *trans* as revealed by the strong absorption band near 920 cm^{-1} (not shown). It can be assigned to the symmetric C–C–$N(CH_3)_3$ stretching vibration of the *trans* conformer (39). This feature disappears completely in the liquid state reflecting the increase of conformational freedom of the TMA-moiety. This result is confirmed by the N–$(CH_3)_3$ antisymmetric stretching band which protrudes as a broad feature at 3027 cm^{-1} in the liquid phase (not shown). In the crystalline state the methyl stretching vibration splits, however, into three clearly resolved peaks at 3008, 3017, and 3031 cm^{-1} probably due to the nonequivalence of the three methyl groups and of their antisymmetric C–H stretches in an immobilized structure (40).

DISCUSSION

Molecular Origin of Hydration Enthalpies

Extensive work has been devoted in the past to the molecular origin of amphiphilic hydration (2–5, 41). On the one hand, hydration phenomena can be attributed to the properties of the water subphase (4, 5, 16, 42). For example, the water molecules are assumed to orient within the electric field of the surface dipoles and local excess charges of the headgroups (42). On the other hand, hydration is viewed as a solvation phenomenon that causes several disordering processes within the lipid aggregates such as, e.g., the increase in the flexibility of the headgroups and undulations of the polar surface (1, 6). In a general sense, "hydration" means the creation of a polar/apolar interface between the water and the hydrocarbon chains of the amphiphiles. It represents the net result of an intricate interplay between different inter- and intramolecular interactions. Each of them will contribute to the enthalpy of the system. Let us express the enthalpies of the amphiphile, h_L, and of its hydration shell, $R_{W/L} \cdot h_W^s$, in terms of intermolecular pair-interaction energies, $u_{X\text{-}Y}$, and of the intramolecular energy of the amphiphile, u_{intra} (see Eq. [13] and Fig. 2 for illustration):

$$h_L \approx u_L = u_{CH\text{-}CH} + u_{HG\text{-}HG} + U_{W\text{-}HG} + u_{intra} \quad \text{and}$$
$$R_{W/L} \cdot h_W^s \approx U_W = U_{W\text{-}W} + U_{W\text{-}HG} \quad [15]$$

with

$$u_{CH\text{-}CH} = \frac{1}{2}\langle \sum_{i \neq j}^{N_L} u_{CH\text{-}CH}^{ij} \rangle_i;\ u_{HG\text{-}HG} = \frac{1}{2}\langle \sum_{i \neq j}^{N_L} u_{HG\text{-}HG}^{ij} \rangle_i$$

$$U_{W\text{-}W} = \sum_{j}^{R_{W/L}} u_{W\text{-}W}(j);\ U_{W\text{-}HG} = \sum_{j}^{R_{W/L}} u_{W\text{-}HG}(j)$$

$$u_{W\text{-}W}(j) = \frac{1}{2}\langle \sum_{j \neq k}^{N_W} u_{W\text{-}W}^{jk} \rangle_i;\ u_{W\text{-}HG}(j) = \frac{1}{2}\langle \sum_{k}^{N_L} u_{W\text{-}HG}^{jk} \rangle_i. \quad [16]$$

We consider interactions between the hydrocarbon chains (subscript CH-CH), between the headgroups (HG-HG) and between the water molecules (W-W). For the sake of simplicity, only cross interactions between the water and the headgroups (W-HG) within the polar region of the molecular aggregates are taken into account. The angular brackets denote ensemble averaging over the amphiphiles. The $u_{X\text{-}Y}^{ij}$ terms include dispersive, electrostatic, and "chemical" interactions such as hydrogen bonding. Making use of $h_W^s = \partial(H_{sample}/N_L)/\partial R_{W/L}$, $h_W^b \approx u_{W\text{-}W}^b$, and of Eqs. [13], [15], and [16] one obtains the change of the partial molar enthalpy of water on hydration as the sum of the energy terms:

$$\Delta h_W^{b \to s} \approx u'_{CH} + u'_{HG} + \Delta U_W$$

with

$$u'_{CH} = u'_{CH\text{-}CH} + u'_{intra}, \quad u'_{HG} = u'_{HG\text{-}HG} + U'_{W\text{-}HG} + u_{W\text{-}HG},$$

and

$$\Delta U_W = U'_{W\text{-}HG} + U'_{W\text{-}W} + (u_{W\text{-}HG} + u_{W\text{-}W}^s - u_{W\text{-}W}^b) \quad [17]$$

The terms within the parentheses $(\cdots)$ give the change in interaction energies of the transferred water. The derivatives, $(\cdots)' \equiv \partial(\cdots)/\partial R_{W/L}$, express the fact that the transfer of a differential quantity of water potentially perturbs the interactions within whole system sorbent + sorbate due to intermolecular couplings.

Interactions within the Polar Region of the Aggregates

The wavenumbers of the IR absorption bands of the carbonyl and the phosphate groups of the lipid continuously shift upward at dehydration indicating the subtle variation of water–lipid interactions (cf. Fig. 10). The blue shift of these stretching vibrations can be attributed to a weakening of the corresponding interaction term, i.e., $u'_{HG} < 0$ (cf. Eq. [17] and Fig. 12 for illustration), although the magnitude of this energy change is difficult to assess.

Because of sterical arguments the water molecules which desorb at $R_{W/L} > 4.5$–5.5 (POPC) and $R_{W/L} > 1.5$–2.5 (DTAB) can be assumed to possess no direct contacts with the headgroups. The corresponding energy changes of the headgroups are probably mediated through the water molecules of the primary hydration shell which bind directly to the headgroups via H bonds and/or they are due to long-range electrostatic interactions arising, e.g., from the dipole potential of the membrane. Also the melting/freezing hysteresis of DTAB is obviously correlated to a solvent mediated influence of the second hydration layer on the arrangement of the detergent molecules. Note that DTAB instantly imbibes water up to $R_{W/L} > 3$ at the melting transition whereas chain freezing starts only at $R_{W/L} < 2$, i.e., after the removal of the water which directly interacts with the headgroups.

At $R_{W/L} < 4.5$–5.5 (POPC) and $R_{W/L} < 2$–2.5 (DTAB) direct interactions between the headgroups are expected to replace water–headgroup contacts when water is removed from the interface. In fact, the considerable shift of the $\nu_{as}(PO_2^-)$ absorption bands of POPC gives strong indication that H bonds between water and the phosphate groups are progressively broken up at dehydration (38). It is known that the phosphate groups tend to interact directly with the trimethylammonium (TMA) groups at a low level of hydration (13, 43). The hydrogen bonds between the water and the PO_4^- moiety can, however, not be replaced by energetically equivalent interac-

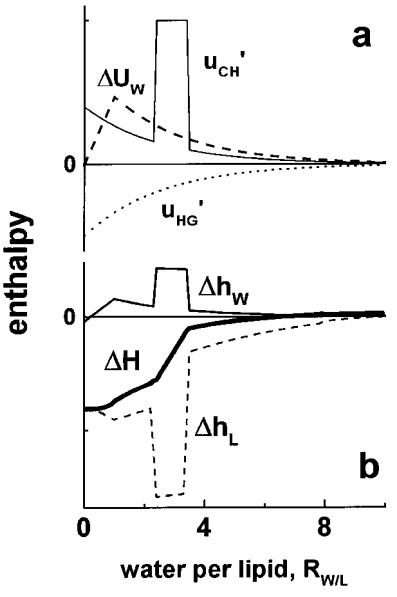

FIG. 12. Schematic representation of the contributions of the water, ΔU_W, of the headgroups, u'_{HG}, and of the acyl chains, u'_{CH}, of POPC (a) to the partial molar enthalpy of water, $\Delta h_W^{b\to s}$ (b, solid line), which is drawn together with the partial molar enthalpy of the lipid, $\Delta h_L^{b\to s}$ (dashed), and the integrated enthalpy of dehydration, $\Delta H^{s\to b}$ (thick solid line). See Eq. [17] and text for explanation.

tions between the polar moieties of the lipid. Its formation leads to a loss of energy of the phosphate groups (3) because TMA–phosphate interactions do not possess the characteristics of hydrogen bonding. On the other hand, the water dipoles associate with the charged TMA moieties via relatively weak polar interactions (38, 44). Therefore the TMA groups energetically gain slightly when replacing the polar TMA–water with stronger TMA–phosphate contacts (43). Despite this fact, the overall enthalpic balance of the PC group is suggested to become progressively exothermic in terms of $\Delta h^{b\to s}$ as illustrated schematically in Fig. 12 (i.e., $0 > u'_{HG}$).

The measured heats possess, however, opposite sign when compared with this expectation, i.e., $\Delta h_W^{b\to s} > 0$. Hence, the energetic loss of the PC group upon dehydration is obviously overcompensated by the endothermic contribution of the hydrocarbon chains, $u'_{CH} > 0$, and/or of the water, $\Delta U_W > 0$ (cf. Eq. [17]). The right-hand shift of the ν_{13}(OH) absorption band upon dehydration has been suggested to reflect the strengthening of the interaction energies of water (cf. Fig. 11). Apparently, the change of this IR parameter contradicts the measured heats. Note however that the ν_{13}(OH) band virtually represents a spectroscopic average over the energetic characteristics of the water molecules sorbed. Local effects such as the strong H bonding between selected water molecules and the phosphate oxygens of the lipid can give the leading contribution to the spectral shift. As a consequence, the ν_{13}(OH) frequency must not necessarily correlate with the mean enthalpy of the water.

On the other hand, one should take into account that the ν_{13}(OH) spectrum shown in Fig. 11 corresponds to $R_{W/L} \approx 1$, i.e., to the first water molecule which binds on the average to each lipid molecule. It can be assumed to interact preferentially with the phosphate moiety which is known to represent the primary hydration site of lipids with PC headgroups. Quantum-chemical calculations yield interaction energies of water bound to $(CH_3)_2PO_4^-$ ranging from -110 to -43 kJ/mol (45, 46) whereas the energy gain from the association of water with, e.g., $N^+(CH_3)_4$ is distinctly smaller, $-(40–30)$ kJ/mol (47). These values agree with the results of computer simulations of water sorbed onto PC headgroups (48). It was found that the first two water molecules interact strongly with the phosphate moiety with $u_{W\text{-}HG}(1) \approx u_{W\text{-}HG}(2) < -70$ kJ/mol. Hence, the maximum position of the ν_{13}(OH) band at $R_{W/L} \approx 1$ can be in fact interpreted as an indication of the stronger binding of the first water when compared with the next ones. Unfortunately, the precision of the calorimetric data decreases considerably at $R_{W/L} < 2$ (cf. Fig. 8), and thus the reliable estimation of the respective interaction energies is prevented at present by the uncertainty of the method.

To summarize, strong H bonds of the water to one or several binding sites of the headgroups do obviously not compensate for the overall endothermic enthalpic balance accompanying the hydration of the amphiphiles. It should be concluded that it is the entropy which drives hydration by an overcompensation of the enthalpic penalty. Hence, solvating water molecules probably screen direct interactions between the headgroups leading to the increase in their conformational and/or motional freedom. Molecular dynamics simulations show that, e.g., polarization due to water molecules almost completely cancel the polarization due to lipid headgroups, and thus the water obviously behaves like a classical medium with high dielectric constant (44, 46, 48, 49).

The Hydrophobic Region: Thermodynamics of the Lyotropic Melting Transition

The position of the stretching bands of the polar moieties and of the methylene groups of POPC shift in opposite directions upon dehydration (cf. Fig. 10). The effective shift of the $\nu_{as}(CH_2)$ band in the fluid and gel states of lipids depends on the balance between repulsive and attractive contributions to the intermolecular potential and on the conformation of the hydrocarbon chain, i.e., on $u_{CH\text{-}CH}$ and on u_{intra}, respectively (50). Measurements at increasing hydrostatic pressure have shown that the wavenumber of the CH_2 stretching bands decreases at pressures up to ~0.5 GPa but increases at higher pressures (31). Attractive or repulsive interactions seem to dominate the respective compression ranges. The water activities which are used to dehydrate the amphiphiles correspond to a hydration pressure, $\Pi = -RT \cdot \ln a_W/v_W$, of up to ~0.5 GPa ($v_W \approx 1.8 \times 10^{-5}$ m^3/mol, the molar volume of water). Recently, we found that the methylene stretching frequency is directly proportional to the area requirement of lipid molecules at the water/air interface, A_L (51). Note that the attractive

TABLE 1
Thermodynamic Data of the Lyotropic Melting Transition of POPC and DTAB

	Gravimetry[a]					ITC[b]			DSC[c]	
Method: System	ΔR_m	μ_W^m (kJ/mol)	$\Delta H_m^{g\to b}$ (kJ/mol)	ΔH_m (kJ/mol)	ΔG_m (kJ/mol)	ΔH_m (kJ/mol)	ΔS_m (J/mol · K)	ΔQ_{ITC}^m (kJ/mol)	ΔH_m (kJ/mol)	ΔS_m (J/mol · K)
POPC	0.4 ± 0.1	-2.34	-18 ± 4	19 ± 3	-0.9	17 ± 3	60	0 ± 1	15 ± 1[d]	50[d]
DTAB hydr.scan	3.2 ± 0.2	-0.46	-143 ± 10	33 ± 10	-1.4	18 ± 10	92	-125 ± 5	10 ± 1	33
DTAB dehydr.scan	1.5 ± 0.2	-1.44	-67 ± 10	21 ± 10	-1.6	17 ± 10	99	-50 ± 5	14 ± 1	49

[a] See Appendix.
[b] $\Delta H_m^{ITC} = -\Delta H^{s\to b}$(fluid) $- \Delta H^{s\to b}$(solid) and $\Delta S_m^{ITC} = (\Delta H_m^{ITC} - \Delta G_m)/T_m$; $T = 25$°C.
[c] Measured at constant $R_{W/L} = 3$; $\Delta S_m = \Delta H_m/T_m$. The rows "hydration" and "dehydration" scans of DTAB refer to heating and cooling, respectively. The corresponding transition temperatures are $T_m = 33$ and 15°C, respectively.
[d] G. Klose, H. Binder, and H. Pfeiffer, to be submitted.

van-der-Waals potential between parallel CH_2 chains is related to the mean molecular cross section by a $\propto A_L^{-3}$ dependence. These facts give rise to the conclusion that the red shift of $\nu_{as}(CH_2)$ at dehydration reflects the continuous decrease of $u_{CH\text{-}CH}$ and of u_{intra} as well, because lateral compression increases the conformational order of the polymethylene chains. Hence, the hydrophobic core is expected to give a progressively increasing endothermic contribution to $\Delta h_W^{b\to s}$ as illustrated in Fig. 12.

The melting transition of the amphiphiles represents the most prominent structural change observed. Humidity titration calorimetry detects this event as an endothermic peak when displaying the transfer enthalpy of hydration, $\Delta h_W^{b\to s}$, as a function of $R_{W/L}$ (cf. Fig. 8). This result is reasonable because the accompanying *trans–gauche* isomerization consumes energy (i.e., $u'_{intra} > 0$, cf. Eq. [18]). The increment of the integrated enthalpy of dehydration at the phase transition gives the corresponding transition enthalpy, $\Delta H_{ITC}^m = \Delta H^{s\to b}$(fluid) $- \Delta H^{s\to b}$(solid) (see Fig. 9). Table 1 compares these values with the transition enthalpies which are obtained by (i) the application of the Clausius–Clapeyron relation to the temperature shift of the lyotropic phase transition (see Appendix) and (ii) by DSC measurements on definitely hydrated amphiphiles. The results of the three independent methods agree within the error limits.

The melting of the hydrocarbon chains is accompanied by the adsorption of $\Delta R_m = 0.4$–3 water molecules per amphiphile (cf. Figs. 6 and 7 and Table 1). This fact obviously reflects the increased exposure of the polar residues of the amphiphiles to the water in the fluid phase. The Clausius–Clapeyron relation predicts $\Delta R_m > 0$ if the water activity of the phase transition, a_W^m, decreases with increasing temperature in agreement with the experimental findings (see Appendix).

The free energy decreases at the chain melting transition by $\Delta G^m \approx -(1$–$2)$ kJ/mol owing to the adsorption of water (see Appendix, Eq. [A2], and Table 1). Note that the endothermic transition enthalpy, ΔH_m, is overcompensated by a positive entropic contribution, $T\Delta S_m$, to yield $\Delta G_m < 0$. The enthalpy and entropy of melting of long chain compounds depend nearly linearly on the number of methylene groups per molecule, n_{chain} (52). The almost equal ΔS_{ITC}^m values of DTAB ($n_{chain} = 12$) and of POPC ($n_{chain} = 28$) show that the entropic effect per CH_2 segment is much more pronounced for the detergent. This difference can be rationalized by the fact that DTAB transforms from a more ordered solid (crystals) into a more disordered fluid (micelles) state when compared with the gel and liquid-crystalline phases of the lipid (30) (vide supra).

Interestingly, the melting/freezing hysteresis of the detergent has no significant effect on ΔS_m and ΔH_m. That means that the arrangement of the alkyl chains in the crystals before melting/after freezing seems to be similar although the scan direction gives rise to a pronounced variation of water binding.

The integral heat which is measured in the ITC experiment at the melting transition, $\Delta Q_{ITC}^m = Q_{ITC}$(fluid) $- Q_{ITC}$(solid), can be understood as the balance of two enthalpic contributions, namely the heat which is released upon condensation of gaseous water onto the headgroups and the heat which is consumed by the hydrocarbon chains to transform into a more disordered state (cf. Eqs. [8]). The phase transition of POPC proceeds without significant net heat effect, i.e., $\Delta Q = \Delta Q_{ITC}^m \approx 0$ (cf. Fig. 7). The exothermic heat of water binding obviously compensates the endothermic heat of chain melting essentially in this special case. For DTAB the former effect exceeds the latter considerably and, thus, the calorimeter records intense CFB pulses when the system passes the phase transition (cf. Figs. 4 and 6). Table 1 lists the heat $\Delta H_m^{g\to b}$ which corresponds to the condensation of ΔR_m water molecules onto bulk water. The transition enthalpy of the amphiphiles is given to a good approximation by $\Delta H_m \approx \Delta Q_{ITC}^m - \Delta H_m^{g\to b}$.

"Range and Strength" of Hydration

Equation [10] transforms the water activity into the energetic scale of the free enthalpy of dehydration, $\Delta G^{s\to b}$. Figure 13

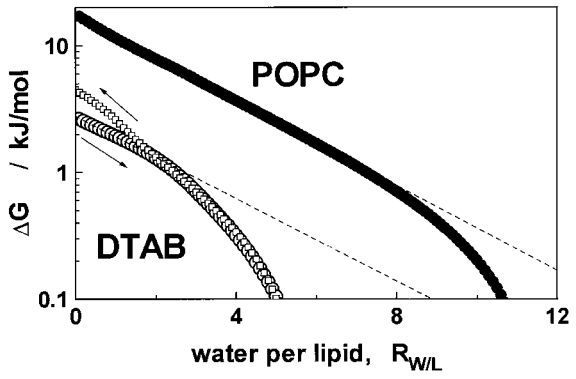

FIG. 13. Free energy of dehydration, $\Delta G^{s\to b}$ (cf. Eq. [10]) of POPC (●) and of DTAB (○, hydration scan; □, dehydration scan) as a function of water molecules per amphiphile, $R_{W/L}$ ($T = 25°C$). The lines are linear regressions for $R_{W/L} < 6$ (POPC) and <3 (DTAB, see Table 2).

depicts $\Delta G^{s\to b}$ in a logarithmic representation as a function of $R_{W/L}$. The fit of

$$\Delta G^{s\to b} = \Delta G_0 \cdot \exp\left(-\frac{R_{W/L}}{R^0_{W/L}}\right) \qquad [19]$$

to the experimental data at $R_{W/L} < 6$ (POPC) and <3 (DTAB) yields the corresponding free enthalpy of complete dehydration, ΔG_0, and the decay constant, $R^0_{W/L}$, which gives a characteristic number of tightly bound water molecules within the range of primary hydration (cf. Table 2).

The free energy of total dehydration, ΔG_0, and the expenses of free enthalpy to remove the first water from the amphiphiles, $\Delta G(1)$, differ considerably between the lipid and the detergent (Table 2). The nearly equal values of $R^0_{W/L}$ seem to, however, contradict the potency of the PC groups to form H bonds to the water in contrast to the $N^+(CH_3)_3$ sites of DTAB. Hence, this parameter is obviously not directly correlated to the strength of local headgroup–water interactions. $R^0_{W/L}$ characterizes the decay of the free enthalpy of dehydration. It represents therefore a measure of the work that has to be applied to remove water from the amphiphiles. It includes enthalpic (energetic) and entropic contributions as well. The exponential decay law [19] describes the hydration of a number of lipids with different headgroups (2). $R^0_{W/L}$ decreases considerably from values about $\sim 2.8 \pm 0.3$ to $\sim 1.8 \pm 0.3$ when the methyl groups of the TMA moiety of lipids with a PC headgroup were replaced by hydrogens (2). The smaller values of $R^0_{W/L}$ correlate with the fact that the corresponding phosphatidylethanolamine (PE) headgroups form a rigid network which does not require water molecules owing to the formation of direct H bonds between the ammonium and phosphate groups (53).

In contrast, the TMA and PC moieties are not stabilized by H bonds in the anhydrous state. Their nearly equal $R^0_{W/L}$ values can be understood if this parameter reflects the potency of water to solvate ("lubricate") the headgroups. If one considers that $R^0_{W/L}$ is directly proportional to the decay length of the repulsive "hydration" forces acting between polar interfaces (2) then our interpretation is in correspondence with that of Israelachvili and Wennerström (6) who stated that "genuine" hydration effects in fact determine the hydrated sizes of polar groups but probably play only an indirect role in the interaction between amphiphilic surfaces. It seems to be more akin to steric repulsion which is caused by entropic effects.

SUMMARY AND CONCLUSIONS

It is demonstrated that isothermal titration calorimetry can be successfully applied to study the thermodynamics of the adsorption of a gaseous sorbate onto a sorbent existing in a liquid-crystalline or solid phase. We have presented a humidity titration technique to investigate hydration phenomena of amphiphilic molecules such as lipids and detergents. This method yields the partial molar enthalpy of water on adsorption as a function of the number of water molecules bound per amphiphile.

The amphiphiles assemble into aggregates the physical state of which depend on the degree of hydration. Consequently the sorbent + sorbate system has been considered as a binary mixture where the enthalpy of both components varies upon changing the composition.

The lyotropic melting of the hydrocarbon chains unequivocally demonstrates that water adsorption onto amphiphiles is not an effect which is only localized to the polar/apolar interface but it involves the whole amphiphilic aggregates including the hydrophobic core. The lyotropic phase transition can be understood in terms of an enthalpic balance where the exothermic heat of adsorption is partially or completely consumed by the hydrocarbon chains upon melting.

Typically, the amphiphiles are dispersed in water. It is therefore convenient to compare the enthalpy of adsorption with the condensation heat of water to characterize the hydration of the amphiphiles in an aqueous environment thermodynamically. It turns out that hydration of DTAB and POPC at

TABLE 2

Free Enthalpy of Complete Dehydration, ΔG_0, Decay Constant $R^0_{W/L}$ and $\Delta G(1)$, the Free Enthalpy of the First Water[a] Bound to POPC and DTAB (cf. Eq. [19] and Fig. 13)

	ΔG_0 (kJ/mol)	$R^0_{W/L}$	$\Delta G(1)$ (kJ/mol)
POPC	17 ± 2[b]	2.6 ± 0.2	5.4[b]
DTAB (hydration scan)	2.8 ± 0.3	2.7 ± 0.2	0.9
DTAB (dehydration scan)	5.2 ± 0.5	2.1 ± 0.3	2.0

[a] $\Delta G(1) = \Delta G^{s\to bulk}(0) - \Delta G^{s\to bulk}(1) \approx \Delta G_0 \cdot (1 - \exp(1/R^0_{W/L}))$ (cf. Eq. [19]).

[b] ΔG_0 and $\Delta G(1)$ increase to 25 and 8 kJ/mol, respectively, if one assumes that 1 water cannot be removed by the drying procedure used (vide supra).

room temperature is endothermic because the water on the average looses enthalpy upon binding to the headgroups of the amphiphiles investigated. One can suggest that the steric restriction and the polarization of the surface prevents the formation of a network of hydrogen bonds such as in bulk water. Hydration appears to be driven by the gain of entropy which accompanies the disordering of the polar and apolar regions of the aggregates.

APPENDIX

Variation of Thermodynamic Functions at the Lyotropic Phase Transition

The molar free energy of the hydrated amphiphile is given by $G = \mu_L + R_{W/L} \cdot \mu_W$. The liquid and solid phases coexist at the water activity, a_W^m, at which the phase transition takes place. The thermodynamic criterion of phase coexistence requires equal chemical potentials of the water and the lipid in the coexisting phases, i.e.,

$$\mu_L^{solid} = \mu_L^{liquid} \quad \text{and}$$
$$\mu_W^m = \mu_W^{solid} = \mu_W^{liquid} = \mu_W^b + RT \cdot \ln(a_W^m). \quad [A1]$$

The variation of $\Delta G^{s\to b}$ at the phase transition,

$$\Delta G_m^{solid\to liquid} \equiv \Delta G^{s\to b}(liquid) - \Delta G^{s\to b}(solid)$$
$$= \Delta R_{W/L}^{solid\to liquid} RT \cdot \ln(a_W^m), \quad [A2]$$

is solely caused by the adsorption of $\Delta R_m \equiv \Delta R_{W/L}^{solid\to liquid}$ water molecules because of $\Delta\mu_L = \Delta\mu_W^m = 0$. This process corresponds to a condensation heat of

$$\Delta H_m^{g\to b} = \Delta R_m \cdot \Delta h_W^{g\to b} \quad [A3]$$

which would be released if the adsorbed water behaves enthalpically like bulk water ($\Delta h_W^{g\to b} = -44.6$ kJ/mol at 25°C). The chain melting is first order and, thus, the changes of the extensive parameters of the system are related to the phase coexistence line by the Clausius–Clapeyron relation

$$\frac{\Delta\Pi_m}{\Delta T_m} = \frac{\Delta S_m}{\Delta V_m}, \quad [A4]$$

where $\Delta\Pi_m = R(T_{m1} \cdot \ln a_W^{m1} - T_{m2} \cdot \ln a_W^{m2})/v_W$ is the shift of the hydration pressure of the phase transition upon varying the temperature by $\Delta T_m = T_{m1} - T_{m2}$. Assuming volumetrically incompressible amphiphiles the change of the volume at the phase transition is given by the volume of the adsorbed water $\Delta V_m \approx \Delta R_m \cdot v_W$ ($v_W = 1.8 \times 10^{-5}$ m^3/mol, the molar volume of water). Insertion into Eq. [A4] and making use of $\Delta G_m = \Delta H_m - T_m \Delta S_m$ yields the enthalpy change at the phase transition

$$\Delta H_m = \Delta R_m \cdot R \cdot \{T_m \cdot \ln a_W^m + \Delta T_m^{-1} \cdot (T_{m1} \ln a_W^{m1} - T_{m2} \ln a_W^{m2})\}. \quad [A5]$$

ACKNOWLEDGMENT

We thank Prof. Schmiedel for valuable comments. This work was supported by the Deutsche Forschungsgemeinschaft under Grant SFB294/C7.

REFERENCES

1. Cevc, G. J., *Chem. Soc. Faraday Trans.* **97,** 2733 (1991).
2. Rand, R. P., and Parsegian, V. A., *Biochim. Biophys. Acta.* **988,** 351 (1989).
3. Cevc, G. *in* "Water and Biological Macromolecules" (E. Westhof, Ed.), p. 368. CRC Press, Boca Raton, FL, 1993.
4. Marcelja, S., and Radic, N., *Chem. Phys. Lett.* **42,** 129 (1976).
5. Kornyshev, A. A., and Leikin, S., *Phys. Rev. A.* **40,** 6431 (1989).
6. Israelachvili, J. N., and Wennerström, H., *J. Phys. Chem.* **96,** 520 (1992).
7. Heerklotz, H., and Binder, H., *Recent Development Phys. Chem.* **1,** 221 (1997).
8. Wiseman, T., Williston, S., Brandts, J. F., and Lin, L. N., *Anal. Biochem.* **179,** 131 (1989).
9. Heerklotz, H., Binder, H., Lantzsch, G., and Klose, G., *J. Phys. Chem. B.* **101,** 639 (1997).
10. Heerklotz, H., Binder, H., and Schmiedel, H., *J. Phys. Chem. B.* **102,** 5363 (1998).
11. Mädler, B., Binder, H., and Klose, G., *J. Coll. Interface Sci.* **202,** 124 (1998).
12. Binder, H., Anikin, A., Kohlstrunk, B., and Klose, G., *J. Phys. Chem. B.* **101,** 6618 (1997).
13. Binder, H., Gutberlet, T., Anikin, A., and Klose, G., *Biophys. J.* **74,** 1908 (1998).
14. Binder, H., Anikin, A., Lantzsch, G., and Klose, G., *J. Phys. Chem. B.* **103,** 461 (1999).
15. Binder, H., Kohlstrunk, B., and Heerklotz, H. H., *Chem. Phys. Lett.* **304,** 329 (1999).
16. Parsegian, V. A., Fuller, N., and Rand, R. P., *Proc. Nat. Acad. Sci. USA.* **76,** 2750 (1979).
17. Pohle, W., Selle, C., Fritzsche, H., and Binder, H., *Biospectroscopy* **4,** 267 (1998).
18. Binder, H., Kohlstrunk, B., Brenn, U., Schwieger, W., and Klose, G., *Colloid Polym. Sci.* **276,** 1098 (1998).
19. Ruthven, D. M., "Principles of Adsorption and Adsorption Processes." Wiley, New York, 1984.
20. Elworthy, P. H., *J. Chem. Soc.*, 4897 (1962).
21. Kelker, H., and Schumann, C. "Handbook of Liquid Crystals." Verlag Chemie, Weinheim, 1980.
22. Larsson, K., "Lipids-Molecular Organization, Physical Functions and Technical Applications." The Oily Press, Dundee, 1993.
23. Cameron, D. G., and Mantsch, H. H., *Biophys. J.* **38,** 175 (1982).
24. Kobayashi, M., Kobayashi, T., Cho, Y., and Kaneko, F., *Makromol. Chem. Macromol. Symp.* **5,** 1 (1986).
25. Jendrasiak, G. L., and Hasty, J. H., *Biochim. Biophys. Acta.* **337,** 79 (1974).
26. Klose, G., König, B., and Paltauf, F., *Chem. Phys. Lipids.* **61,** 265 (1992).
27. Bechinger, B., and Seelig, J., *Chem. Phys. Lipids.* **58,** 1 (1991).
28. Snyder, R. G., Strauss, H. L., and Elliger, C. A., *J. Phys. Chem.* **86,** 5145 (1982).

29. Casal, H. L., and Mantsch, H. H., *Biochim. Biophys. Acta.* **779,** 381 (1984).
30. Cevc, G., and Marsh, D. "Phospholipid Bilayers. Physical Principles and Models." Wiley, New York, 1987.
31. Siminovitch, D. J., Wong, P. T. T., Berchtold, R., and Mantsch, H. H., *Chem. Phys. Lipids.* **46,** 79 (1988).
32. Benson, A. M., and Drickamer, H. J., *J. Chem. Phys.* **27,** 1164 (1957).
33. Blume, A., Hübner, W., and Messner, G., *Biochemistry.* **27,** 8239 (1988).
34. Arrondo, J. L. R., Goni, F. M., and Macarulla, J. M., *Biochim. Biophys. Acta.* **794,** 165 (1984).
35. Zundel, G., "Hydration of Intermolecular Interactions." Academic Press, New York, 1969.
36. Grdadolnik, J., Kidric, J., and Hadzi, D., *J. Mol. Structure.* **322,** 93 (1994).
37. Walrafen, G. E., *J. Chem. Phys.* **55,** 768 (1971).
38. Wong, P. T. T., and Mantsch, H. H., *Chem. Phys. Lipids.* **46,** 213 (1988).
39. Fringeli, U. P., and Günthard, H. H., *Mol. Biol. Biochem. Biophys.* **31,** 270 (1981).
40. Derreumaux, P., Wilson, K. J., Vergoten, G., and Peticolas, W. L., *J. Phys. Chem.* **93,** 1338 (1989).
41. Helfrich, W., *Z. Naturf. A* **33,** 305 (1978).
42. Cevc, G., and Marsh, D., *Biophys. J.* **47,** 21 (1985).
43. Grdadolnik, J., Kidric, J., and Hadzi, D., *Chem. Phys. Lipids.* **59,** 57 (1991).
44. Zhou, F., and Schulten, K., *J. Phys. Chem.* **99,** 2194 (1995).
45. Frischleder, H., Gleichmann, S., and Krahl, R., *Chem. Phys. Lipids.* **19,** 144 (1977).
46. Peinel, G., Frischleder, H., and Binder, H., *Chem. Phys. Lipids.* **33,** 195 (1983).
47. Port, G. N., and Pullman, A., *Theoret. Chim. Acta.* **31,** 231 (1973).
48. Klose, G., Arnold, K., Peinel, G., Binder, H., and Gawrisch, K., *Colloids Surf.* **14,** 21 (1985).
49. Binder, H., and Peinel, G., *J. Mol. Structure.* **123,** 155 (1985).
50. Guo, J. D., and Zerda, T. W., *J. Phys. Chem. B.* **101,** 5490 (1997).
51. Binder, H., Dietrich, U., Schalke, M., and Pfeiffer, H., *Langmuir* **15,** 4857 (1999).
52. Small, D. M., "The Physical Chemistry of Lipids." Plenum Press, New York/London, 1986.
53. Hitchcock, P. B., Mason, R., Thomas, K. M., and Shipley, G. G., *Proc. Nat. Acad. Sci. USA.* **71,** 3036 (1974).